Co-published by
Institute of Fluid-Flow Machinery
Polish Academy of Sciences
and
Committee on Thermodynamics and Combustion
Polish Academy of Sciences

http://www.imp.gda.pl/archives-of-thermodynamics/

ARCHIVES OF THERMODYNAMICS

Effect of flow orientation in experimental studies on FC-770 boiling heat transfer in asymmetrically heated minichannels

Magdalena Piasecka[a*], Kinga Strąk[a]

[a]Kielce University of Technology, al. Tysiaclecia Panstwa Polskiego 7, PL-25-314 Kielce, Poland
*Corresponding author email: tmpmj@tu.kielce.pl

Received: 31.12.2023; revised: 25.03.2024; accepted: 30.04.2024

Abstract

The article presents experimental results of boiling heat transfer during FC-770 flow in a group of five minichannels with a common heated wall. The flow orientation was changed from 0º to 180º, with a 15° increment. During the experiments, the temperature of its outer heated wall surface was measured by an infrared camera. At the same time, flow patterns were captured through the glass plate opposite the heated wall using a high-speed camera. The purpose of the calculations was to determine local heat transfer coefficients on the contact surface between the working fluid and the heated surface in the central minichannel, using a simplified 1D calculation method. The results in the form of dependences of the temperature of the heated wall and the heat transfer coefficient as a function of the distance from the channel inlet for various flow orientations were analysed. Furthermore, typical boiling curves and two-phase flow patterns were presented. The mean relative error of the heat transfer coefficient was determined for various flow orientation. The dependence of the void fraction as a function of heat flux was illustrated for various angles of minichannel inclination to the horizontal plane. It was observed that the void fraction increased with heat flux and with increasing angle of inclination of the minichannel to the horizontal plane.

Keywords: Heat transfer; Flow boiling; Minichannel; Flow orientation; Flow pattern

Vol. 45(2024), No. 2, 29–39; doi: 10.24425/ather.2024.150849

Cite this manuscript as: Piasecka, M., & Strąk, K. (2024). Effect of flow orientation in experimental studies on FC-770 boiling heat transfer in asymmetrically heated minichannels. *Archives of Thermodynamics*, 45(2), 29–39.

1. Introduction

Due to the rapid advancement of modern technologies, the miniaturisation of devices and components is progressing in engineering applications. Reliable and efficient heat transfer in flowing fluids is crucial in various industrial processes, including high-power electronics, microelectronics, IT microprocessors, and microfluidics. The study of flow boiling heat transfer in small-dimension channels is of great interest to scientists, especially for cooling miniature high-power components. Many research centres are investigating factors that influence the intensification of heat transfer, particularly during phase change processes such as boiling and condensation. One significant aspect under investigation is the impact of different orientations of the heat exchanger on the heat transfer coefficient.

A brief review of the literature on flow boiling heat transfer during refrigerant flow in channels of small dimensions.

In [1], an experimental study was conducted to investigate

Nomenclature

A – channel cross-sectional area, m^2
G – mass flux, kg/(m^2·s)
I – current, A
MRE_α – mean relative error of the heat transfer coefficient, %
ONB – onset of nucleate boiling
p – pressure, Pa
q_w – heat flux (density), W/m^2
T – temperature, K
T_s – ambient temperature, K
x – distance from the minichannel inlet along the direction of flow, m

Greek symbols

α – heat transfer coefficient, W/(m^2·K)
α_s – heat transfer coefficient at the interface between the heated wall and the surroundings, W/(m^2·K)
Δ – absolute error
ΔT_{sub} – inlet liquid subcooling, K, $\Delta T_{sub} = T_{sat,in} - T_{f,in}$
ΔU – voltage drop, V
δ – thickness, m
λ – thermal conductivity, W/(m·K)

Subscripts and Superscripts

f – fluid
in – at the inlet
$loss$ – heat loss
sat – saturation
w – heated wall

bubble dynamics and flow patterns during flow boiling of HFE-7000 in high aspect ratio microchannels of various channel orientations. The test section utilized a transparent glass minichannel with a width-to-height aspect ratio of 10 and a hydraulic diameter of 909 μm. The channel received uniform heating, and a tantalum layer coating facilitated observations. The study focused on the growth of a single bubble and the influence of mass flux and heat flux on bubble behaviour. Additionally, the paper explored the impact of channel orientation on bubble behaviour, considering aspects such as bubble evolution, shape, and nose velocity. No significant differences in flow patterns were observed when comparing horizontal and vertical upward orientations. The study identified two types of instabilities associated with the dominant flow pattern during flow boiling.

Considering the same test section with channels of 5 mm width and 0.5 mm depth, authors in [2] addressed the pressure and thermal characterization of dynamic instabilities during flow boiling of FC-72, exploring different channel orientations. One-sided heating at various channel orientations relative to gravity was considered, ranging from bottom heating (0°) to top heating (180°) in 30° increment. For each channel orientation, the study examined various combinations of heat flux and mass flux leading to categorized flow instabilities. Generally, orientations with a horizontally heated surface (0° and 180°) were more susceptible to flow instability, while intermediate azimuthal rotations (30°, 60° and 90°) showed flow instability only at the highest mass flow rates. At the highest mass flow rates, the horizontal orientation of 180° and heating from the top showed an increase in the heat transfer coefficient (during instability) of up to 77% and 275% in single-phase and two-phase regions, respectively, compared to stable initial conditions.

The authors of [3] discussed modifications to the inlet and outlet plenum, as well as the outlet port orientations, to address instabilities in two-phase microchannel heat sinks. The study explored four orientations: horizontal flow (+0°), downward-facing horizontal flow with downward orientation (–0°), and vertically aligned upward (+90°) and downward flows (–90°). The orientation of the inlet-outlet port was perpendicular to the plane of the microchannel footprint area. As a result, the study proposed straightforward guidelines for designing the inlet and outlet plenum, as well as port orientations, to mitigate instabilities in two-phase microchannel heat sinks, especially at high heat fluxes and under unfavourable orientations.

In [4], upward flow boiling heat transfer of HFE-7000 in a vertical tube under a high-frequency alternating-current electric field was investigated. The test section was coated with a 600 nm transparent indium tin oxide layer, enabling visual access to boiling dynamics within the tube while simultaneously serving as an electrical heater element for heat transfer. The experiments were carried out under constant mass flux and inlet subcooling, varying heat flux, voltages, and at three frequencies (100 Hz, 1 000 Hz, and 10 000 Hz). At 100 Hz frequency, the study observed a heat and mass transfer phenomenon, resulting in a more than two-fold enhancement in heat transfer at low heat fluxes.

In [5], the influence of minichannel geometrical configuration on flow structures, hydrodynamics, and heat transfer behaviour in a FC-72 cooling system with high heat flux during subcooled flow boiling was presented. Two-dimensional numerical simulations were conducted for two different configurations (straight and periodic constriction-expansion) of a minichannel mounted vertically, maintaining constant mass and input heat flux, and varying three inlet temperatures. The results in both configurations showed that with an increase in the inlet temperature, the heat transfer coefficient also increased. The periodic constriction-expansion configuration exhibited the greatest enhancement in heat transfer (21.77–36.9%) for an inlet temperature range from 285.35 K to 325.35 K.

Experimental research on flow boiling bubble motion under an ultrasonic field in a vertical minichannel, utilizing a bubble tracking algorithm, was presented in [6]. The central component of the experimental system was the minichannel section with a heat sink. The heat sink featured 14 rectangular minichannels with a length of 220 mm, width of 2 mm, and height of 2 mm, using R141b fluid as the working fluid. It was observed that the use of ultrasound significantly increased the detachment frequency, speed, and bubble travel distance, leading to an extremely unstable two-phase gas-liquid flow. Numerical simulations were employed to quantitatively investigate the movement mechanism of bubbles in microchannels under the influence of

an ultrasonic field.

In [7], a thorough investigation was conducted into the thermo-hydrodynamic effects of the minichannel configuration on the thermal performance of subcooled flow boiling. The study focused on cooling using FC-72 at high heat flux values in various vertical minichannel shapes. Particular attention was given to developing a numerical approach to predict highly subcooled flow. The computational results were validated through experimental measurements, revealing notable agreements that highlighted the effectiveness of the numerical model. The results demonstrated a decrease in the heat transfer coefficient with increasing mass flux, and the design with expanding shapes improved thermal efficiency by up to 24.68% and 10.45% compared to straight and expanding shapes, respectively.

The investigation of flow boiling heat transfer in FC-72 fluid within a vertical rectangular narrow minichannel was presented in [8]. The studies were focused on two-phase flow patterns and a local void fraction. The dimensions of the minichannel were 0.5–1.5 mm in depth, 20 mm in width and 360 mm in length. The results indicated that the local heat transfer coefficient increased with increasing pressure within the channel and this effect was observed under varying mass flux conditions.

In the study [9], flow boiling heat transfer of R1233zd(E) was investigated in a 3 mm vertical circular minichannel at moderate and high saturation temperatures. In particular, all heat transfer trends initially decreased with increasing vapour quality but later stabilised or even increased because of convective boiling effects. The experimental data were compared with predictions from an in-house model and established two-phase flow correlations known from the literature. It was underlined that the in-house model demonstrated the highest accuracy, with a mean absolute percentage error of 23.17% for R1233zd(E) and 19.23% for R245fa.

In [10], the authors investigated boiling heat transfer during R134a flow in a single horizontal circular tube with a diameter of 5 mm. Key findings include that the heat transfer coefficient decreases as the vapour quality increases, sensitivity to heat flux is observed, but is insensitive to mass flux, and sensitivity to vapour quality at low values. Furthermore, nucleate boiling dominates in regions with low vapour quality. Additionally, the study mentions new environmentally friendly low-pressure refrigerants based on fluorocarbons.

Several new environmentally friendly low-pressure refrigerants from fluorocarbon and hydrofluoroether (HFE) groups used in investigations of heat transfer during flow in minichannels were presented in [11]. The authors present the most important properties and applications of refrigerants of these groups and review the literature on their use. In the results, HFE refrigerants show better thermal properties than the Fluorinert FC-72.

In [12], saturated flow boiling in a one-sided heated rectangular microchannel was examined. The working fluid used was deionised water. The primary focus of the investigation was on local heat transfer coefficients, pressure drop and flow patterns for surfaces with various wettability characteristics. The bottom surface was a hydrophilic bare silicon wafer with a contact angle of 65°. In contrast, a superhydrophilic surface was created by depositing a 100 nm thick silicon dioxide film, resulting in a contact angle of less than 5°. The experiments involved a range of mass fluxes from 120–360 kg/(m^2s) and inlet vapour qualities between 0.03 and 0.1. Flow visualisation revealed local dry out on the untreated hydrophilic surface at high heat fluxes and low mass fluxes, leading to a decrease in heat transfer performance. However, this phenomenon was not observed on the superhydrophilic surface under the same conditions. The hydrophilic surface experienced significant heat transfer deterioration with increasing inlet vapour quality, while the heat transfer coefficient of the superhydrophilic surface remained relatively constant. A similar investigation was described in [13]. The authors concluded that the superhydrophilic surface maintained relatively constant heat transfer performance because of the continuous and uniform distribution of the thin liquid film on the heated surface during annular flow dominance. This delayed the onset of partial dryout, resulting in superior performance compared to the untreated hydrophilic surface, without any additional pressure drop penalty.

Authors of [14], discussed a method for studying two-phase heat transfer in mini and microtubes. The focus was on the evaporation of a thin liquid film. The study used the Tikhonov regularisation method to solve the inverse heat conduction problem in the tube wall, providing a way to estimate local convective wall heat flux and heat transfer coefficients. The temperature distributions on the outer surface of the channel, measured by an infrared camera, were taken as input data to solve this inverse problem. The results confirm existing correlations in the average values.

Conducting heat transfer calculations for flow boiling in minichannels was a main topic reported in [15]. The experimental setup was the same as was applied in this article, consisting of five parallel mini-channels, sharing a common heated wall. Temperature measurements were taken using K-type thermoelements and an infrared camera in selected mini-channels to estimate temperature uncertainty. The results from the Monte Carlo simulation method were compared with those from the uncertainty propagation method. The main experiment was conducted to investigate heat transfer in the subcooled boiling region. Local heat transfer coefficients at the interface between the working fluid and the heated wall were calculated using the Robin boundary condition. The mathematical model, described by the heat equation in the mini-channel wall and the Fourier-Kirchhoff equation in the flowing fluid, led to an inverse heat transfer problem. This problem was solved using the Finite Element Method with Trefftz-type basis functions. The final results of the heat transfer coefficient included the estimation of temperature uncertainty measurements from the Monte Carlo method.

Numerous publications have explored research on the pool boiling process involving various working fluids and using developed heated surfaces. References [16–18] and [19] cover various aspects of this topic. In [16] a study was presented on pool boiling heat transfer of water and ethanol using two types of structures prepared on the samples by laser treatment. Research on pool boiling of FC-72 on open surfaces with parallel microchannels made of copper was reported in [17]. Furthermore in [18] explores pool boiling heat transfer process of FC-72 on

open surfaces with microchannels while [19] investigates the same issue related to enhanced heated wall surfaces with mesh structures and microfins.

In general, the authors' previous work focused on boiling heat transfer during flow in a single minichannel at various inclinations relative to the horizontal plane, including 0º, 45º, 90º, 135º, and 180º, using FC-72 as a working fluid [20]. Experiments carried out in a vertical and horizontal minichannel with FC-72, HFE-649, HFE-7000, or HFE-7100 circulated in the main loop were discussed in [21]. Additionally, the results of experiments involving seven inclinations of the test section with a minichannel (0°, 30°, 60°, 90°, 120°, 150°, and 180°) and three refrigerants as working fluids, namely FC-72, HFE-7100, and HFE-7000, were analysed in [22]. The main findings included intensification of heat transfer during flow in minichannels and observation of flow patterns. The novelty of the presented work lies in the assessment of the intensity of flow boiling heat transfer during the flow of Fluorinert FC-770 in a group of five asymmetrically heated minichannels. Another goal is to compare the results of temperature and heat transfer coefficient as the flow direction changes within the orientation range from 0° to 180° with a 15° increment. This helps identify positions that ensure a high intensity of heat transfer processes.

2. Experimental setup

2.1. Research rig

The experiments were carried out using a research rig comprising the main circulation loop with FC-770, the data and image acquisition system equipped with the lighting system, and the power supply and control system, as shown in Fig. 1.

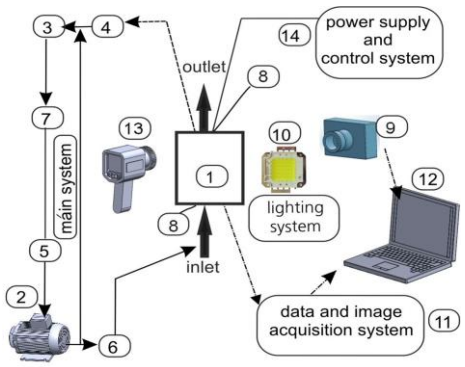

Fig. 1. A schematic diagram of the main systems on the research rig: 1 – a test section; 2 – a gear pump, 3 – a pressure regulator, 4 – a heat exchanger, 5 – a filter, 6 – a Coriolis mass flowmeter, 7 – an air separator, 8 – a pressure meter, 9 – a high-speed camera, 10 – LED lighting system, 11 – the data and image acquisition system, 12 – a PC, 13 – an infrared camera, 14 – the power supply and control system with heat source.

The flow loop consists of: a test section with a group of five minichannels (1), a gear pump (2), a pressure regulator (3), a heat exchanger (4), a filter (5), a Coriolis mass flowmeter (6), an air separator (7), pressure meters (8), a high-speed camera (9) and an infrared camera (13). Detailed information on all elements of the research rig is provided in [23].

2.2. Test section and its spatial orientation

The test section, which features a group of five asymmetrically parallel and rectangular heated minichannels, is a crucial component of the setup, as shown in Fig. 2. Each minichannel has a cross-section of 1 mm x 6 mm, sharing a common heated wall approximately 0.1 mm thick, made of Haynes-230 alloy. The working fluid was FC-770 (Fluorinert™ FC-770, 3M). Table 1 provides the main thermal and flow properties of the Fluorinert FC-770. The experimental series were conducted under stationary conditions with a constant mass flow rate and a slight overpressure.

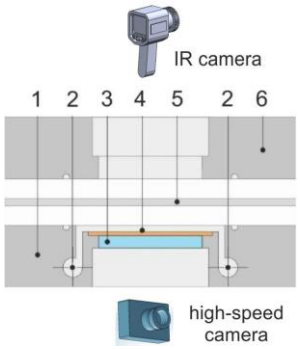

Fig. 2. Schematic of the test section (longitudinal section): 1 – channel body, 2 – inlet/outlet chamber, 3 – glass plate, 4 – minichannel, 5 – heated wall, 6 – top cover.

Table 1. Main properties of Fluorinert™ Electronic Liquid FC-770.

Main properties (units)	Values
Boiling point (K)	368
Heat of vaporization (J/kg)	85.9×10^3
Liquid density (kg/m³)	1793
Vapour pressure (Pa)	6.568×10^3
Thermal conductivity (W/(m·K))	0.063
Kinematic viscosity (m²/s)	0.79×10^3
Coefficient of expansion (1/K)	0.00148
Molecular weight (kg/kmol)	399
Surface tension (N/m)	0.0148

The exterior surface of the heated wall of the minichannels was coated with black paint to achieve an emissivity of 0.83. The temperature of this heated wall surface was measured using an A655SC infrared camera (manufactured by FLIR). The axially symmetric part of the central minichannel was considered for temperature measurements. A high-speed video camera, SP-5000M-CXP2 (manufactured by JAI), recorded the two-phase flow structures through the glass wall of the minichannels, illuminated by high-power LEDs. The temperature (measured with K-type thermocouples) and pressure (measured with pressure metres) of the working fluid were recorded in the inlet and outlet manifolds of the test section. Furthermore, the electrical parameters of the resistance heated wall were captured.

The spatial orientation of the test section and the direction of the fluid flow in the minichannels varied from 0° to 180°, with an increment of 15°, as schematically illustrated in Fig. 3. The

research considered 13 different positions of the test section in relation to the horizontal plane: one vertical with upward flow of the fluid (90°), two horizontal (the position named 0° while the fluid flows above the heated wall, and the other position named 180° while the heated wall was above the fluid), and ten other positions between them. It should be emphasised that the test section is asymmetrically heated.

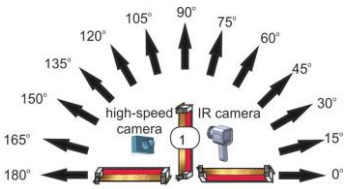

Fig. 3. A scheme of spatial orientation of the test section showing the direction of the fluid flow in minichannels, 1 – the test section with minichannels.

2.3. Experimental methodology, thermal and flow parameters

Fluorinert FC-770 was circulated in the flow loop. During each experiment, the mass flux was stabilised at the constant value, low overpressure was established, and test section was spatially oriented according to the research schedule.

The main experimental thermal and flow parameters of the experimental sets selected for the analyses are listed in Table 2.

Table 2. Main thermal and flow parameters of the experimental sets.

Main thermal or flow parameters	Values / Ranges of values
Heat flux, q_w (kW/m²)	33.3-63.9
Mass flux, G (kg/(m²·s))	145
Inlet pressure, p_{in} (kPa)	103-183
Inlet liquid subcooling, ΔT_{sub} (K)	79.3-101.6

Throughout each series of tests, the subcooled liquid enters the minichannels and heats up as it flows towards the outlet along the heated wall. The heat flux supplied to the heated wall of the minichannels is gradually increased. The heat transfer process converts from single-phase forced convection to subcooled boiling, finally achieving saturated boiling. At the outlet, a two-phase liquid-vapour mixture emerges, directed subsequently to the additional heat exchanger, the condenser.

3. Determination of the heat transfer coefficient and mean relative error

3.1. The heat transfer coefficient

The heat transfer coefficient calculations were performed using a simple 1D calculation method applied to the central channel of the group of five. In this method, only one direction of heat flow was considered, taking into account the primary direction of heat flow perpendicular to the direction of the fluid flow in the channel [23].

Local values of the heat transfer coefficient were calculated using Newton's law:

$$\alpha(x) = \frac{q_w}{T_w(x,\delta_w) - T_f(x)}, \tag{1}$$

where q_w is the heat flux transferred from the heated wall to the fluid, x – distance from the minichannel inlet, along the direction of flow, $T_w(x,\delta_w)$ – the temperature at the heated wall – fluid interface, δ_w – thickness of the minichannel heated wall, T_f – the temperature of the fluid, calculated locally based on measured temperatures at the inlet and the outlet of the minichannel (with the assumption of a linear dependence of the fluid temperature from the inlet to the outlet).

The heat transferred to the fluid in the minichannel was assumed to be equal to the difference between the heat generated by the heated wall and the heat loss to the surroundings:

$$q_w = \frac{I\Delta U}{A_w} - q_{w,loss}, \tag{2}$$

where I – current supplied to the heated wall, ΔU – voltage drop across the heated wall, A_w – surface area of the heated wall, $q_{w,loss}$ – heat loss to the surroundings.

The heat loss to the surroundings was calculated similarly as in previous work [22], according to the following dependence:

$$q_{w,loss} = \alpha_s \cdot [\max T_w(x) - T_s], \tag{3}$$

where α_s – the heat transfer coefficient at the interface between the heated wall and the surroundings, T_w – temperature of the outer surface of the minichannel heated wall registered by an infrared camera, T_s – ambient temperature.

The temperature at the heated wall–fluid interface was calculated as follows:

$$T_w(x,\delta_w) = T_w(x) - q_w \frac{\delta_w}{\lambda_w}, \tag{4}$$

where λ_w – thermal conductivity of the minichannel heated wall.

Finally, local values of the heat transfer coefficient at the subcooled flow boiling region were determined from the following formula:

$$\alpha(x) = \frac{\frac{I\Delta U}{A_w} - q_{w,loss}}{T_w(x) - T_f(x) - \left(\frac{I\Delta U}{A_w} - q_{w,loss}\right)\cdot\frac{\delta_w}{\lambda_w}}. \tag{5}$$

3.2. The mean relative error of the heat transfer coefficient

The mean relative error of the heat transfer coefficient MRE_α was estimated from the following formula:

$$MRE_\alpha = \frac{\sqrt{\left(\frac{\partial\alpha(x)}{\partial T_w(x)}\Delta T_w(x)\right)^2 + \left(\frac{\partial\alpha(x)}{\partial T_f(x)}\Delta T_f(x)\right)^2 + \left(\frac{\partial\alpha(x)}{\partial\lambda_w}\Delta\lambda_w\right)^2 + \left(\frac{\partial\alpha(x)}{\partial\delta_w}\Delta\delta_w\right)^2 + \left(\frac{\partial\alpha(x)}{\partial q_w}\Delta q_w\right)^2}}{\alpha(x)} \tag{6}$$

The absolute errors of components, needed to calculate MRE_α according to the dependence (6) are listed in Table 3.

Table 3. The absolute errors of components of the dependence (6) for determining of MRE_α.

Components in Eq. (6) for determining of MRE_α	Absolute errors
Thermal conductivity of the minichannel heated wall	$\Delta\lambda_w$ = 0.1 W/(m·K)
Thickness of minichannel heated wall	$\Delta\delta_w = 5\times10^{-5}$ m
Temperature of the outer surface of the minichannel heated wall registered by an infrared camera	$\Delta T_w(x)$ = 2.0 K
Heated wall area	$\Delta A_w = 2.8\times10^{-5}$ m^2
Current intensity supplied to the minichannel heated wall	ΔI = 0.18 A
Voltage drop across the minichannel heated wall	$\Delta(\Delta U)$ = 0.02 V
Fluid temperature difference between the temperatures measured by thermocouples at the minichannel inlet and outlet	$\Delta T_f(x)$ = 0.34 K [24]

It should be underlined that each of the two K-type thermocouples (one installed at the inlet and the other at outlet of the minichannels) was additionally calibrated with the use of a temperature calibrator, which was described in detail in [24].

The absolute error of the heat flux Δq_w was determined for the lowest value of the heat flux supplied to the heated wall of the minichannels (q_w = 33.3 kW/m^2). The absolute error of the heat flux was found to be 0.83%. The procedure for calculating the absolute error and the relative error of the heat flux was similar to that reported in [22].

The mean relative errors of the heat transfer coefficient MRE_α, obtained for various flow orientations of the test section, are shown in Table 4.

Table 4. The mean relative error of the heat transfer coefficient MRE_α for various flow orientation.

Spatial orientation of the test section (°)	The mean relative error of the heat transfer coefficient MRE_α (%)
0	3.28
15	3.28
30	3.36
45	3.42
60	2.90
75	3.23
90	3.32
105	3.24
120	3.24
135	3.23
150	3.35
165	3.30
180	3.50

When analysing the values of the mean relative errors of the heat transfer coefficient (MRE_α), listed in Table 4, it was observed that in the subcooled boiling region, they are low, ranging from 2.90% to 3.50%. The lowest MRE_α was achieved for the 60° position, while the highest values were observed for the 180° position. These results are consistent with findings from previous studies, as presented, for example, in [21,22].

4. Results

4.1. Main description

The results are presented in Figs. 4–9 in the form of:

- dependencies of the minichannel heated wall temperature (measured by an infrared camera) as a function of distance from the inlet, for two heat fluxes – Fig. 4;
- dependencies of the heat transfer coefficient as a function of distance from the inlet, for two heat fluxes – Fig. 5;
- dependencies of the heat transfer coefficient as a function of flow orientation of the minichannel at two distances from the inlet, for two heat fluxes – Fig. 6;
- images of two-phase flow patterns characteristic for analysed flow orientations – Fig. 7;
- boiling curves, based on the data collected during the experiments carried out for various flow orientations, for two distances from the inlet – Fig. 8,
- dependencies of the void fraction as a function of heat flux, prepared on the basis of recorded two-phase flow images during experiments at various flow orientations, for one distance from the inlet – Fig. 9.

In Fig. 4 the results for two values of the heat flux supplied to the heated wall in the subcooled boiling region (q_w = 46 kW/m^2 and q_w = 64 kW/m^2) were shown as local temperatures of the outer surface of the heated wall, obtained from measurements due to infrared thermography.

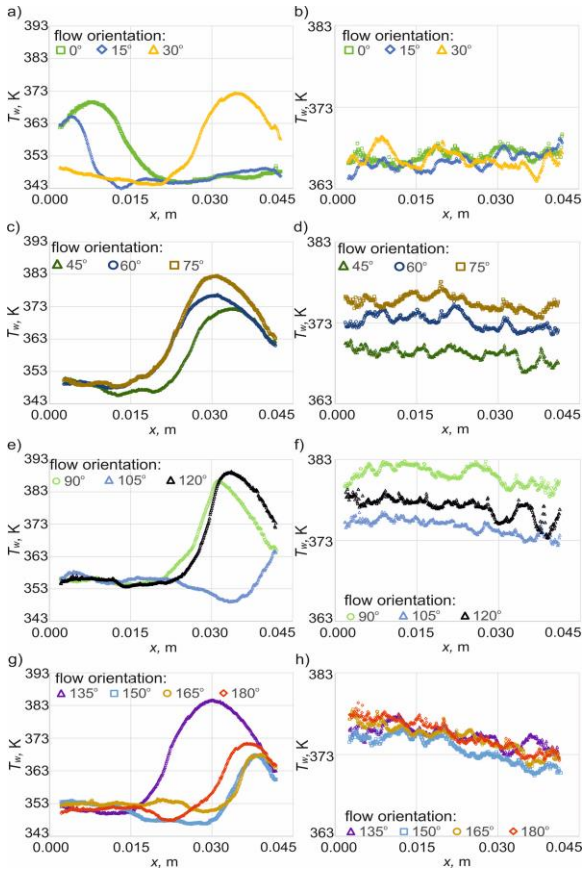

Fig. 4. Dependencies of the minichannel heated wall temperature measured by an infrared camera (T_w) as a function of distance from the inlet (x) for analysed flow orientations, at two heat fluxes (q_w): 46 kW/m^2 (a, c, e, g) and 64 kW/m^2 (b, d, f, h).

The local heat transfer coefficients corresponding to these temperature data are illustrated in Fig. 5. Both dependences are given as functions of the distance from the minichannel inlet.

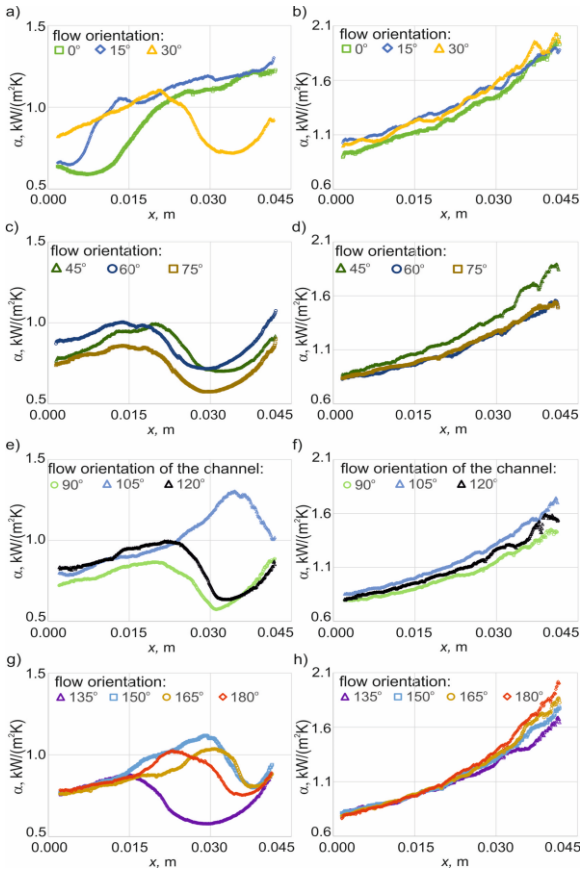

Fig. 5. Dependencies of the heat transfer coefficient (α) as a function of distance from the inlet (x) for the analysed flow orientations, at two heat fluxes (q_w): 46 kW/m^2 (a, c, e, g) and 64 kW/m^2 (b, d, f, h).

Furthermore, the dependence of the heat transfer coefficient and the flow orientation of the minichannel are presented in Fig. 6, at two locations: one-third distance and two-thirds distance, from the inlet, as the results of the calculations for two heat fluxes.

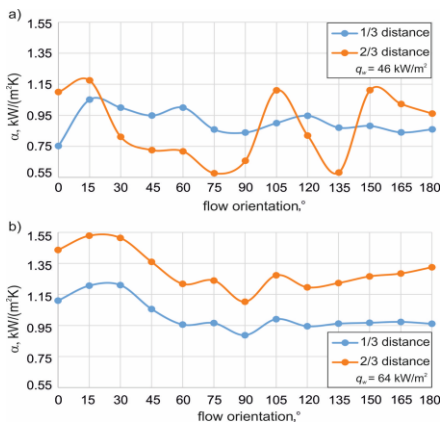

Fig. 6. Dependencies of the heat transfer coefficient (α) as a function of flow orientation, constructed at locations: one-third distance and two-thirds distance from the inlet, for two heat fluxes (q_w): a) 46 kW/m^2 and b) 64 kW/m^2.

For general view, the two-phase flow are shown in Fig. 7 as images of two-phase flow patterns, characteristic for various flow orientations.

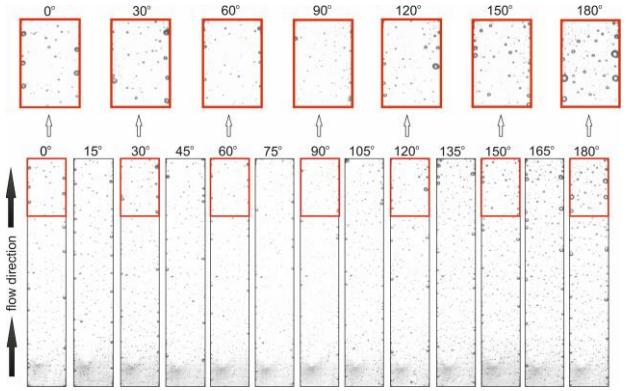

Fig. 7. Images of the characteristic two-phase flow patterns for each of the analysed flow orientations, with enlarged fragments of the outlet area for selected minichannel positions.

The boiling curves are illustrated in Fig. 8, constructed for two distances from the inlet, for all tested spatial orientations of the minichannel.

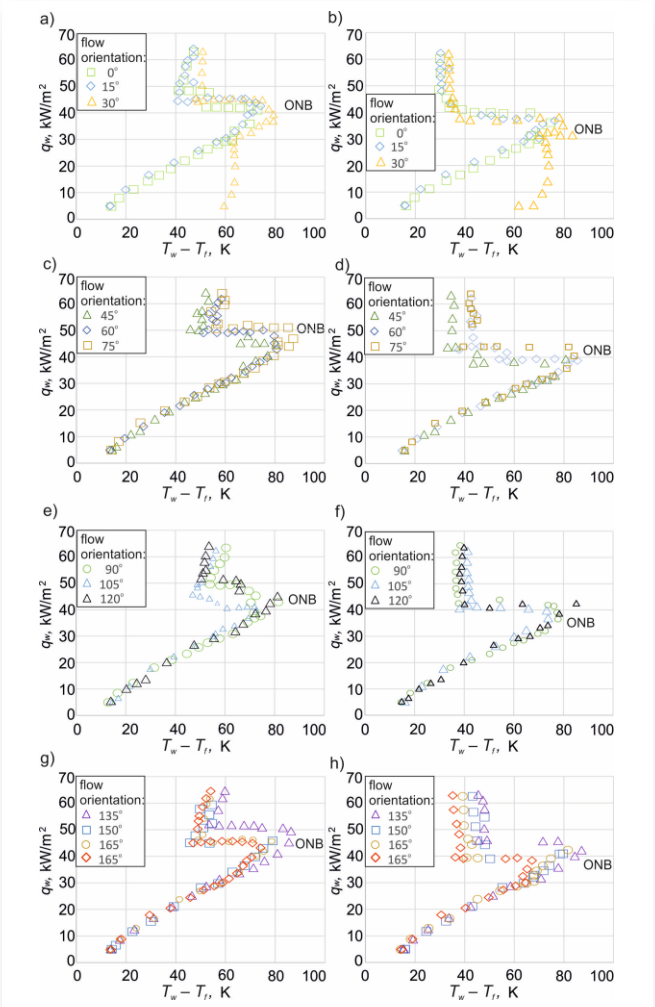

Fig. 8. Boiling curves, based on the data collected during experiments carried out for analysed flow orientations, constructed at locations: one-third distance (a, c, e ,g) and two-thirds distance (b, d, f, h) from the inlet, ONB - onset of nucleate boiling.

In Fig. 9, the relationship between void fraction and heat flux is depicted at a location of two-thirds distance from the inlet.

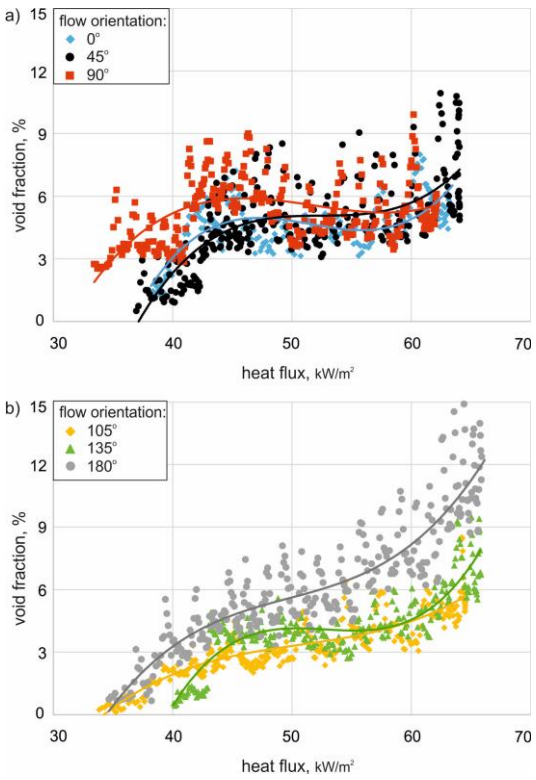

Fig. 9. Void fraction versus heat flux, based on data collected during experiments carried out for selected flow orientations: a) 0°, 45°, 90 °, and b) 105°, 135°, 180°, constructed at a location of two-thirds of the distance from the inlet.

The study described in [25] provides a detailed explanation for determining the procedure for the void fraction. When defining the volumetric void fraction, we consider the proportion of the channel volume filled by the gas phase. Furthermore, for the minichannel, we assume that the two-dimensional area of the vapour is fully occupied by vapour, accounting for the very small third dimension (according to the minichannel depth). Therefore, we provide a cross-sectional void fraction, where the fraction of the channel is assumed to be occupied by the gas phase. Two-phase flow images were performed using a specialist software environment based on LabVIEW functions. Each digital photo was loaded and analysed as a binarized image. To determine the cross-sectional void fraction, the number of pixels corresponding to the gas phase was counted and divided by the total number of pixels in the selected area. For the areas partially filled with vapour, the procedure of closing the bubbles was performed. In the literature on boiling heat transfer, it is common to present thermodynamic vapour quality on the basis of theoretical considerations. However, in this article, the results obtained from the experiments are shown as void fractions, based on the data from the recorded two-phase flow images.

4.2. Observations and analyses

When analysing the temperature distribution on the heated wall surface (Fig. 4), the following observations can be made:

- At a lower heat flux:
  1) The temperature of the heated wall in the outlet part of the minichannel shows a very slight decrease with increasing distance from the inlet (from the inlet up to 1/3 minichannel length), despite the positions of 0° and 15°, for which the diminishing of temperature proceeds much more abruptly;
  2) The temperature of the heated wall increases with distance at the range from 1/3 up to 2/3 minichannel length, reaching a maximum in the end of this range; the highest temperature increase was observed for orientations of 75°, 90°, 120° and 135°, reaching above 385 K while the lowest temperature value was obtained for orientations of 105° and 150°, maximally down to 370 K;
  3) At the outlet part of the minichannel, a diminishing of temperature is noted (despite the position of 105°);

- At a higher heat flux:
  1) The temperature fluctuated very slightly, in comparison with the results obtained for lower heat flux;
  2) The highest values of the heated wall temperature occurred for positions of 90° and 120°;
  3) The lowest temperatures were observed for positions of 0°, 15° and 30°.

When examining the heat transfer coefficient results presented in Fig. 5, several observations can be noted:

- At a lower heat flux:
  1) An increase in the heat transfer coefficient is observed with the distance from the inlet, followed by a decrease in the part of the channel where the highest temperature values were recorded (see Fig. 4), and then a further increase towards the channel outlet;
  2) The heat transfer coefficient values range from 0.5 to 1.4 kW/(m^2·K);
  3) The highest values of the heat transfer coefficient (maximum) are observed for orientations of 0°, 15° and 105°;
  4) The lowest values the heat transfer coefficient (minimum) are seen for orientations of 75°, 90°, 120° and 135°;

- At a higher heat flux:
  1) A clear increase in the heat transfer coefficient is observed along the entire channel length with increasing distance from the inlet;
  2) The values of the heat transfer coefficient are higher in comparison to achieved for lower heat flux, ranging from 0.7 to 2.0 kW/(m^2·K);
  3) The highest values of the heat transfer coefficient are observed for positions of 0°, 15°, 30°, 165° and 180°, reaching a maximum approx. 2.0 kW/(m^2·K);

4) The lowest values of the heat transfer coefficient are obtained for positions of 60°, 75°, and 90° with a maximum of 1.6 kW/(m^2·K).

Upon analysing the results shown in Fig. 6, it is evident that the heat transfer coefficient varies with flow orientation as follows:

- At a lower heat flux (Fig. 6a):
  1) In general, the values of heat transfer coefficients are lower compared to those obtained at higher heat flux, and they are characterised by higher scatter, mainly observed in the results collected at 2/3 distance from the inlet;
  2) The highest values of the heat transfer coefficient at 1/3 distance from the inlet are observed for a position of 15°, while the lowest values are achieved for a position of 0°;
  3) At 2/3 distance from the inlet, the highest values of the heat transfer coefficient are observed also for the position of 15°, while high values are also noted for orientations of 0°, 105°, and 150°; the lowest values are observed for positions of 75° and 135°;
- At a higher heat flux (Fig. 6b):
  1) For both selected distances from the inlet (1/3 and 2/3 distances), similar relationships are obtained, but lower values are noticed at 1/3 distance (it is seen moving down the dependence on the chart by a constant value);
  2) The highest values of the heat transfer coefficient are gained for orientations 15° and 30°;
  3) The lowest values of the heat transfer coefficient are noted for the position of 90° but generally low values are seen in the orientation range 60°–180°.

Describing the two-phase flow patterns illustrated in Fig. 7 for each of the analysed flow orientations, it is emphasized that only a bubbly flow is observed for each channel position. The images show only tiny vapour bubbles, small and uniformly spherical. Larger bubbles can be noticed near the sides of the channels. Moreover, larger spherical bubbles are seen for spatial orientations close to horizontal, where the fluid flows below the heated wall, in the orientation range of 135°–180°.

Boiling curves shown in Fig. 8 are based on the data collected during experiments carried out for analysed flow orientations. The curves were constructed at two selected distances from the inlet (1/3 and 2/3 distances from the inlet), while increasing the heat flux supplied to the heated wall, while heat flux density depends on temperature difference T_w-T_f. The typical shape of the boiling curves is observed. As the heat flux density increases, heat transfer between the heated wall and subcooled liquid flowing in the minichannel occurs through the single-phase forced convection process. The increase in heat flux density activates vapour nuclei on the channel's heated surface. The bubbles formed as a result act as internal heat absorbers, absorbing substantial amounts of energy transferred to the liquid. Spontaneous nucleation causes a drop in the heating surface temperature, while the heat flux density remains nearly constant. This point is marked in the curve course as ONB (onset of nucleate boiling). Further increases in heat flux density lead to developed nucleate boiling [21].

When analysing the courses of the boiling curves presented in Fig. 8, the following observations can be made:

- The boiling curves exhibit a similar course, except for the curve corresponding to 30° in the single-phase forced convection section (Fig. 8a and Fig. 8b);
- The onset of nucleate boiling (ONB) appears at a higher heat flux for the boiling curves generated at the shorter distance from the inlet (1/3 distance) compared to the longer one (2/3 distance), regardless of the flow orientation under consideration;
- The smallest temperature differences are achieved for positions of 0° and 15° (Fig. 8a and Fig. 8b), and for the orientation ranges of 45°–75° and 135°–180°, the highest temperature differences (T_w–T_f) at ONB are observed (Fig. 8c, Fig. 8d and Fig. 8g, Fig. 8h);
- In general, as the angle of flow orientation increases, a higher temperature difference (T_w–T_f) corresponding to ONB occurs for both distances from the inlet;
- For the orientation range of 135°–180°, ONB appears with the highest heat flux compared to other spatial orientations of the test section.

Based on the graphs illustrated in Fig. 9, it was observed that the void fraction increased with rising heat fluxes, as expected. Additionally, it also increased with the increasing angle of inclination of the minichannel to the horizontal plane. The lowest values of void fraction were observed for 0° flow orientation, while the highest values were found for 180° flow orientation (up to 15%).

5. Conclusions

The study investigates boiling heat transfer during the flow of FC-770 in a configuration of five minichannels featuring a shared heated wall. The orientation of the flow was systematically varied from 0º to 180º relative to horizontal plane, with a increment of 15°. Throughout the experiments, an infrared camera monitored the temperature of the outer heated wall, while a high-speed camera captured flow patterns through a glass plate opposite the heated wall. Local heat transfer coefficients on the contact surface between the working fluid and the heated surface in the central minichannel were computed using a simplified 1D calculation method. The results obtained, including the dependencies of the heated wall temperature and the heat transfer coefficient with respect to the distance from the channel inlet for 13 flow orientations, were comprehensively analysed. Additionally, typical boiling curves and two-phase flow patterns were presented and subjected to a thorough discussion. Furthermore, the dependence of the void fraction as a function of heat flux was illustrated for various angles of minichannel inclination to the horizontal plane.

The most important findings cover:

- At a lower heat flux, the temperature of the heated wall reaches a maximum at the outlet part of the channel, and for a higher heat flux, it changes slightly;

- At the lower heat flux, the values of heat transfer coefficients are lower compared to those obtained at higher heat flux, and they are characterised by higher scatter;
- The highest values of the heat transfer coefficient are observed for orientations of 0°, 15° and 105° (at lower heat flux), 0°, 15°, 30°, 165° and 180° (at higher heat flux);
- Analysing the image of flow pattern, the presence of spherical vapour bubbles was observed, with the largest sizes occurring in the orientation range of 135°–180°;
- The initiation of boiling was accompanied by the occurrence of nucleation hysteresis. The typical shape of the boiling curves was observed. The highest temperature difference observed for the orientation ranges of 45°–75° and 135°–180°, and the lowest are achieved for positions of 0° and 15°;
- Void fraction increased with heat flux and also with the increasing angle of minichannel inclination to the horizontal plane, reaching the highest values for 180° flow orientation.

It is crucial to emphasize that boiling processes allow for high heat fluxes with small temperature differences between the heated surface and the working fluid, resulting in high efficiency over a small heat transfer area. Identifying conditions that lead to the most intense flow boiling heat transfer is of paramount importance. The heat transfer coefficient is influenced by various factors, such as thermal and flow parameters, surface roughness, channel geometry, spatial orientation, and properties of the boiling liquid. However, the existing literature on heat transfer in minichannels during flow boiling presents inconsistent results. This underscores the importance of continued research in this field.

Acknowledgments

The research reported herein was supported in part by a grant from Poland's Minister of Education and Science through the Poland's Metrology Programme [Polska Metrologia]. Grant Number: PM/SP/0031/2021/1; Funding: 750 000.00 PLN; Programme budget: 848 200.00 PLN.

References

[1] Widyatama, A., Venter, M., Orejon, D., & Sefiane, K. (2023). Experimental investigation of bubble dynamics and flow patterns during flow boiling in high aspect ratio microchannels with the effect of flow orientation. *International Journal of Thermal Sciences*, 189, 108238. doi: 10.1016/j.ijthermalsci.2023.10823

[2] Vermaak, M., Orejon, D., Dirker, J., Sefiane, K., & Meyer, J.P. (2023). Pressure and Thermal Characterisation of Dynamic Instabilities During Flow Boiling in Micro/Mini-channels at Different Azimuth Orientations. *Applied Thermal Engineering*, 218, 119292. doi: 10.1016/j.applthermaleng.2022.119292

[3] Hedau, G., Qadeer, M., Gulhane, N.P., Raj, R., & Saha, S.K. (2023). On the importance of fluidic manifold design and orientation on flow boiling instability in microchannel heat sinks. *International Journal of Heat and Mass Transfer*, 209, 124120. doi: 10.1016/j.ijheatmasstransfer.2023.124120

[4] Ahmadi, S., Hanafizadeh, P., Eraghubi, M., & Robinson, A.J. (2021). Upward flow boiling of HFE-7000 in high frequency AC electric fields. *International Journal of Thermofluids*, 10, 100076. doi: 10.1016/j.ijft.2021.100076

[5] Igaadi, A., El Amraoui, R., & El Mghari, H. (2023). CFD investigation on heat transfer improvement of subcooled flow boiling in a vertical upflow minichannel with straight and enhanced geometrical structure. *e-Prime - Advances in Electrical Engineering, Electronics and Energy*, 5, 100231. doi: 10.1016/j.prime.2023.100231

[6] Xiao, J., & Zhang, J. (2023). Experimental investigation on flow boiling bubble motion under ultrasonic field in vertical minichannel by using bubble tracking algorithm. *Ultrasonics Sonochemistry*, 95, 106365. doi: 10.1016/j.ultsonch.2023.106365

[7] Igaadi, A., El Amraoui, R., & El Mghari, H. (2024). Thermo-hydrodynamic investigation into the effects of minichannel configuration on the thermal performance of subcooled flow boiling. *Nuclear Engineering and Technology*, 56(1), 265–274. doi: 10.1016/j.net.2023.09.034

[8] Kaniowski, R., & Poniewski, M. (2013). Measurements of two-phase flow patterns and local void fraction in vertical rectangular minichannel. *Archives of Thermodynamics*, 34, 3–21. doi: 10.2478/aoter-2013-0007

[9] Pysz, M., & Mikielewicz, D. (2023). Flow boiling of R1233zd(E) in a 3 mm vertical tube at moderate and high reduced pressures. *Experimental Thermal and Fluid Science*, 147, 110964. doi: 10.1016/j.expthermflusci.2023.110964

[10] Bediako, E.G., Dančová, P., & Vít, T. (2022). Experimental Study of Horizontal Flow Boiling Heat Transfer Coefficient and Pressure Drop of R134a from Subcooled Liquid Region to Superheated Vapor Region. *Energies*, 15, 0681. doi: 10.3390/en15030681

[11] Sikora, M., & Bohdal, T. (2023). New environmentally friendly low-pressure refrigerants mini-channel. *Archives of Thermodynamics*, 44, 89–104. doi: 10.24425/ather.2023.145878

[12] Zhou, K., Coyle, C., Li, J., Buongiorno, J., & Li, W. (2017). Flow boiling in vertical narrow microchannels of different surface wettability characteristics. *International Journal of Heat and Mass Transfer*, 109, 103–114. doi: 10.1016/j.ijheatmasstransfer.2017.01.111

[13] Li, W., Zhou, K., Li, J., Feng, Z., & Zhu, H. (2018). Effects of heat flux, mass flux and two-phase inlet quality on flow boiling in a vertical superhydrophilic microchannel. *International Journal of Heat and Mass Transfer*, 119, 601–613. doi: 10.1016/j.ijheatmasstransfer.2017.11.145

[14] Cattani, L., Bozzoli, F., Ayel, V., Romestant, C., & Bertin, Y. (2023). Experimental estimation of the local heat transfer coefficient for thin liquid film evaporation in a capillary tube. *Applied Thermal Engineering*, 219, 119482. doi: 10.1016/j.applthermaleng.2022.119482

[15] Piasecka, M., Maciejewska, B., & Piasecki, A. (2023). Heat Transfer Calculations during Flow in Mini-Channels with Estimation of Temperature Uncertainty Measurements. *Energies*, 16, 1222. doi: 10.3390/en16031222

[16] Orman, Ł.J., Radek, N., Pietraszek, J., Wojtkowiak, J., & Szczepaniak, M. (2023). Laser Treatment of Surfaces for Pool Boiling Heat Transfer Enhancement. *Materials*, 16(4), 1365. doi: 10.3390/ma16041365

[17] Kaniowski, R., & Pastuszko, R. (2021). Boiling of FC-72 on surfaces with open copper microchannel. *Energies*, 14, 7283. doi: 10.3390/en14217283

[18] Bialek, A., Kargul ,M., & Stokowiec, K. (2023). Boiling heat transfer on porous single layer brass meshes. *Journal of Physics: Conference Series*, 2454, 012004. doi: 10.1088/1742-6596/2454/1/012004

[19] Bialek, A., & Stokowiec, K. (2023). Comparison of boiling heat transfer on heaters with mesh structure and microfins. *Journal of Physics: Conference Series*, 2454, 012005. doi. 10.1088/1742-6596/2454/1/012005

[20] Piasecka, M., & Maciejewska, B. (2015). Heat transfer coefficient during flow boiling in a minichannel at variable spatial orientation. *Experimental Thermal and Fluid Science*, 68, 459–467. doi. 10.1016/j.expthermflusci.2015.05.005

[21] Piasecka, M., Strąk, K., & Maciejewska, B. (2021). Heat transfer characteristics during flow along horizontal and vertical minichannels. *International Journal of Multiphase Flow*, 137, 103559. doi. 10.1016/j.ijmultiphaseflow.2021.103559

[22] Strąk, K., Piasecka, M., & Maciejewska, B. (2018). Spatial Orientation as a Factor in Flow Boiling Heat Transfer of Cooling Liquids in Enhanced Surface Minichannels. *International Journal of Heat and Mass Transfer*, 117, 375–387, doi: 10.1016/ j.ijheatmasstransfer.2017.10.019

[23] Piasecka, M., & Strąk, K. (2022). Boiling Heat Transfer during Flow in Vertical Mini-Channels with a Modified Heated Surface. *Energies*, 15, 7050. doi. 10.3390/en15197050

[24] Piasecka, M., Maciejewska, B., Michalski, D., Dadas, N., & Piasecki, A. (2024). Investigations of Flow Boiling in Mini-Channels: Heat Transfer Calculations with Temperature Uncertainty Analyses. *Energies*, 17, 791. doi. 10.3390/ en17040791

[25] Piasecka, M., Hożejowska, S., Maciejewska, B., & Pawińska, A. (2021). Time-dependent heat transfer calculations with Trefftz and Picard methods for flow boiling in a mini-channel heat sink. *Energies*, 14, 1832. doi. 10.3390/en14071832